

# Bonding rearrangement in amorphous silicon nitrides deposited by hot-wire chemical vapor deposition upon thermal annealing

Y. Mai, V. Verlaan, C.H.M. van der Werf, Z.S. Houweling, R. Bakker, J.K. Rath, R.E.I. Schropp\*

*Utrecht University, Faculty of Science, Department of Physics and Astronomy, SID – Physics of Devices, P.O. Box 80 000, 3508 TA Utrecht, The Netherlands*

Available online 5 February 2008

## Abstract

The bonding rearrangement upon thermal annealing of amorphous silicon nitride ( $a\text{-SiN}_x\text{:H}$ ) films deposited by hot-wire chemical vapor deposition was studied. A wide range of N/Si atom ratio between 0.5 and 1.6 was obtained for the  $a\text{-SiN}_x\text{:H}$  sample series by varying the source gases ratio only. Evolutions of Si–N, Si–H and N–H bonds upon annealing were found to depend strongly on the N/Si atom ratio of the films. According to the above observations, we propose possible reaction pathways for bonding rearrangement in  $a\text{-SiN}_x\text{:H}$  with different N/Si ratios.

© 2008 Published by Elsevier B.V.

*PACS:* 68.60.–p; 68.55.Jk; 78.30.–j; 78.55.Qr

*Keywords:* Silicon; Solar cells; Photovoltaics; Chemical vapor deposition; Rutherford backscattering; FT-IR measurements

## 1. Introduction

Amorphous silicon nitride ( $a\text{-SiN}_x\text{:H}$ ) has been widely used in crystalline silicon (c-Si) solar cells for anti-reflection and surface passivation coatings [1,2]. In addition,  $a\text{-SiN}_x\text{:H}$  provides bulk passivation to the grain boundaries of multi-crystalline silicon (mc-Si) solar cells by atomic hydrogen in-diffusion, which is driven by a high-temperature annealing step, for example a ‘firing’ step [3,4]. Many studies on hydrogen passivation suggest that both the surface and bulk passivation capacity depends critically on the atom densities and bonding structure (such as H content, Si–N bond density, mass density and/or N/Si ratio) of the deposited  $a\text{-SiN}_x\text{:H}$  film [3–7]. To discern the determinative factor of surface and bulk passivation, a systematic study on the bonding rearrangement and H out-diffusion in  $a\text{-SiN}_x\text{:H}$  upon thermal annealing is necessary.

Many researchers have studied the effect of thermal annealing on plasma-deposited  $a\text{-SiN}_x\text{:H}$  [3,8–10]. However, a systematic experiment was seldom carried out for  $a\text{-SiN}_x\text{:H}$  deposited by hot-wire chemical vapor deposition (HWCVD). This is of interest because passivation of mc-Si solar cells by HWCVD  $a\text{-SiN}_x\text{:H}$  has been shown to be as effective as other methods of deposition, while much higher deposition rates can be obtained [7]. In this paper, we report a thermal annealing experiment of a series of  $a\text{-SiN}_x\text{:H}$  with N/Si atom ratio in the wide range from 0.5 to 1.6. It was found that the evolution of Si–N, Si–H and N–H bonds depends critically on the N/Si ratio of the sample.

## 2. Experimental

Eleven  $a\text{-SiN}_x\text{:H}$  films were deposited by HWCVD on c-Si wafers at a substrate temperature of 450 °C. A description of the deposition system can be found elsewhere [11]. The source gases,  $\text{SiH}_4$  and  $\text{NH}_3$ , were catalytically decomposed at four resistively heated tantalum filaments held at 2100 °C, leading to a high deposition rate of about 3 nm/s.

\* Corresponding author.

*E-mail address:* [r.e.i.schropp@uu.nl](mailto:r.e.i.schropp@uu.nl) (R.E.I. Schropp).

The  $\text{NH}_3$  flow was the same for all depositions, while the  $\text{SiH}_4$  flow was varied to obtain different N/Si ratios ranging from 0.5 to 1.6 in the resulting films. The deposition time of each film was deliberately changed to keep the film thickness at about 300 nm. The composition of the deposited samples was determined with elastic recoil detection (ERD) [12] using 50 MeV  $\text{Cu}^{8+}$  ions. Rutherford back scattering (RBS) experiment [13] with 2 MeV  $\text{He}^+$ -atoms was used to accurately determine the mass density. The samples were annealed in a tube oven in a nitrogen atmosphere for different periods of time. The annealing temperature was kept at 800 °C since temperatures around this value are frequently used in the ‘firing’ step for mc-Si solar cell fabrication. The absorption peak intensity and bond configurations of Si–N, Si–H and N–H bonds were evaluated from Fourier transformed infrared (FT-IR) absorption spectra, measured before and after each step of annealing. Corrections for coherent and incoherent reflections were taken care of [14,15] and intensive dry  $\text{N}_2$  purging was used during the FT-IR measurement to minimize the ambient  $\text{H}_2\text{O}$  and  $\text{CO}_2$  signals.

### 3. Results

Under our deposition conditions, film properties, such as hydrogen content ( $C_H$ ), mass density, surface and bulk passivation quality, were found to depend strongly on the N/Si ratio [7,16]. The mass density increased, starting from 2.2  $\text{g}/\text{cm}^3$  at N/Si of 0.5, with increasing N/Si ratio to a maximum of 3  $\text{g}/\text{cm}^3$  at N/Si of  $\sim 1.3$ . From there on it decreased again, down to 2.2  $\text{g}/\text{cm}^3$  as N/Si increased up to  $\sim 1.5$ . Compared to the mass density,  $C_H$  has just an opposite trend and reached its minimum of  $\sim 9$  at.% at N/Si  $\approx 1.3$ .

It was found that the evolutions of Si–H and N–H bonds in a- $\text{SiN}_x\text{:H}$  behave in three different ways upon the thermal annealing, depending on the N/Si ratio. Fig. 1 shows the Si–H and N–H peak intensities of such three typical samples as a function of annealing time. These peak intensities are normalized to the initial values before annealing. (i) In the Si-rich samples with  $\text{N/Si} \leq 1.02$ , both Si–H and N–H peak intensity decreased with the increasing annealing time (see Fig. 1(a) for example). (ii) In the samples close to stoichiometry with  $\text{N/Si} \approx 1.3$ , the N–H peak intensities still decreased with increasing annealing time. However, annealing increased the Si–H peak intensities in the first 4 min and then reduced them slowly afterwards (Fig. 1(b)). (iii) The N-rich samples with N/Si of  $\sim 1.5$  initially had an as-deposited Si–H stretching peak at  $\sim 2210 \text{ cm}^{-1}$ . Annealing reduced this Si–H peak within 4 min. Further annealing, however, introduced a new peak at  $\sim 2175 \text{ cm}^{-1}$ . After 16 min of annealing, the new absorption peak increased up to 5 times stronger than the initial peak at  $\sim 2210 \text{ cm}^{-1}$  and remained almost constant till 60 min (see Fig. 1(c)). It can be seen in Fig. 1 that Si–H and N–H of all types of samples nearly reached saturation after 16 min of annealing at 800 °C.

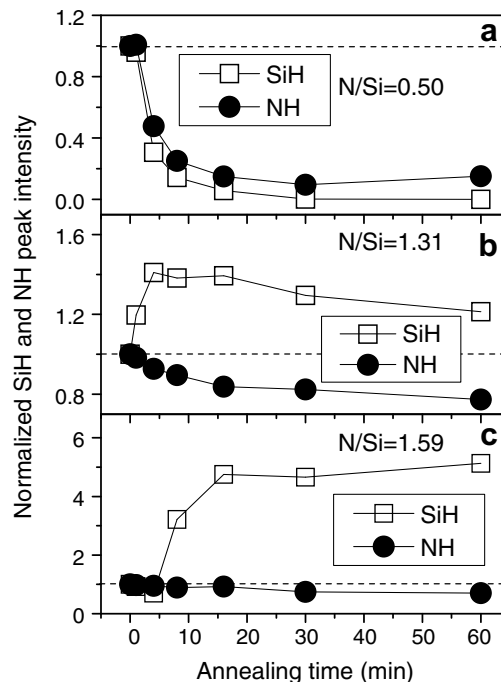


Fig. 1. Normalized Si–H and N–H peak intensities of three typical a- $\text{SiN}_x\text{:H}$  samples with different N/Si ratio.

Therefore, we will mainly show the film properties after 16 min of annealing in the following.

The intensity ratios of Si–H and N–H peaks after thermal annealing relative to the initial peak intensities were found to be N/Si dependent. As can be seen in Fig. 2, more

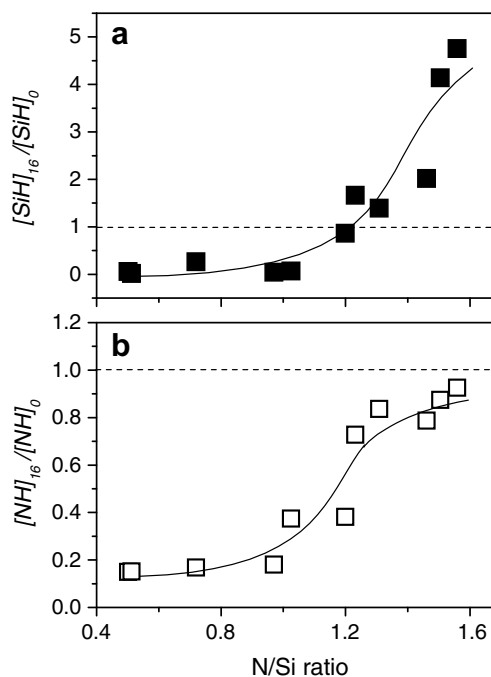


Fig. 2. Ratios of Si–H (a) and N–H peak intensities (b) after 16 min of annealing at 800 °C relative to the initial peak intensities. The data are plotted as a function of N/Si ratio.

N-rich samples maintained relatively more bonded H content in the film after 16 min of annealing.

Fig. 3 shows the Si–H peak positions of the eleven samples before annealing and after 16 min of annealing at 800 °C. The initial Si–H peak position increased almost linearly from  $\sim 2140$  to  $\sim 2220$   $\text{cm}^{-1}$  as N/Si ratio increased from 0.50 to 1.59. Thermal annealing decreased the width of the Si–H peaks and shifted the peak positions to a higher wavenumber in the Si-rich samples with N/Si < 1.02. The newly developed Si–H in the N-rich samples (N/Si of  $\sim 1.5$ ) showed a maximum intensity at  $\sim 2175$   $\text{cm}^{-1}$ , which is about 35  $\text{cm}^{-1}$  smaller than the initial peak position. Thermal annealing hardly changed the Si–H peak position of samples with N/Si of  $\sim 1.3$ . A direct observation in this figure is that Si–H peaks converge to a small range between 2170 and 2200  $\text{cm}^{-1}$  after annealing.

A peak shift of the Si–N peak to higher wavenumber was observed in almost all samples after annealing, indicating a change in the Si–N bonding configuration. Fig. 4 shows the difference between the Si–N peak intensity before and after 16 min of annealing. The contribution of

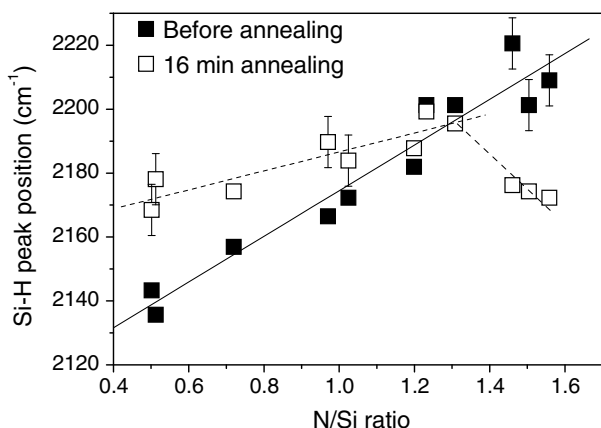


Fig. 3. Peak positions of the Si–H absorption peak before annealing (solid squares) and after 16 min (open squares) of thermal annealing at 800 °C.

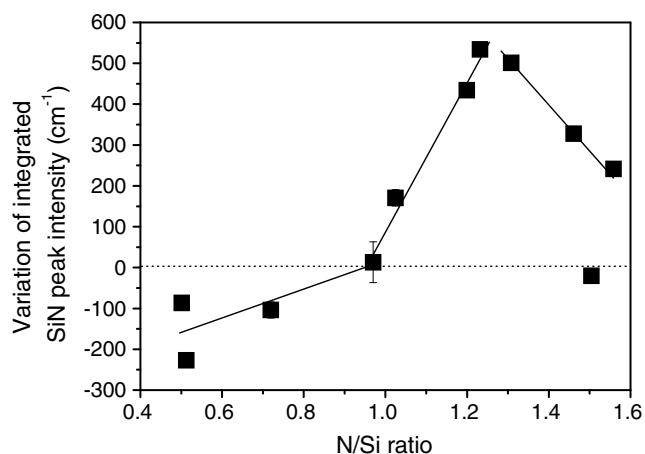


Fig. 4. Sixteen minutes of thermal annealing changed the integrated Si–N peak intensity of the  $\text{a-SiN}_x\text{:H}$  films with different N/Si ratios.

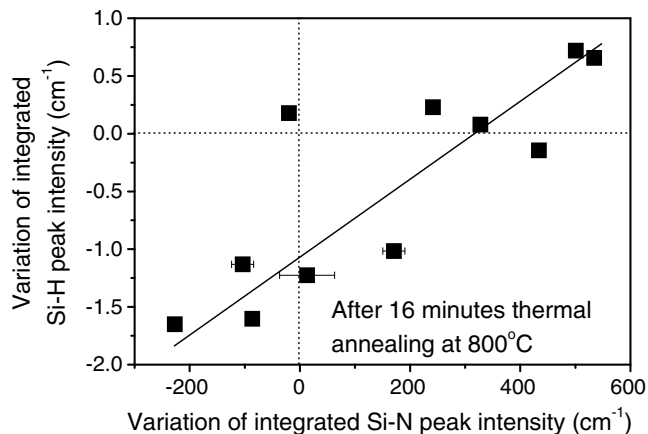


Fig. 5. The absolute variation of Si–H peak intensities after 16 min of annealing at 800 °C versus that of Si–N peak intensities.

the Si–O bond absorption, due to post-deposition oxidation, was carefully eliminated from the Si–N peak intensity calculation. As shown in Fig. 4, annealing for 16 min reduced the Si–N peak intensities of the Si-rich samples with N/Si ratio < 0.72. Amongst the other samples, the most compact  $\text{a-SiN}_x\text{:H}$  with N/Si ratio of  $\sim 1.3$  have the strongest Si–N peak intensity increase. From Fig. 5, an interesting observation is the linear correlation between the variations of the Si–N and Si–H peak intensities, suggesting a close link between the processes of forming or breaking Si–N and Si–H bonds.

#### 4. Discussion

As can be seen above, both Si–H and N–H bonds in Si-rich material with N/Si < 1.02 lose hydrogen during annealing. Reactions including Si–H and N–H bond breaking and  $\text{H}_2$  formation,



were previously proposed for this observation [8–10]. In the most Si-rich sample, the decreased Si–N peak intensities can be ascribed to reactions forming  $\text{NH}_3$  fragments [8].

In order to explain the Si–H increase after annealing in  $\text{a-SiN}_x\text{:H}$  with N/Si > 1.1, reaction



was suggested [8,10,17]. This so-called H migration process, however, was not supported by Savall et al. [9]. They suggested that the enhanced oscillation strength of Si–H bonds after annealing can be attributed to a change in the Si–H bond absorption. Although such large changes in oscillator strength are possible [18], the observations in Fig. 1(c), i.e. the diminishment of the initial Si–H peak and the appearance of a new peak, do not agree with Savall's suggestion. In addition, the linear correlation between the variations of Si–H and Si–N peak intensities (Fig. 5) supports the possibility of reaction (3).

The mass density determined by RBS shows that the a-SiN<sub>x</sub>:H with N/Si close to 1.3 are the most compact. The results in Fig. 2 imply that the H out-diffusion rate is not directly correlated to the compactness of the films, since no correlation between the two is found.

Bustarret et al. [19] suggested that the Si–H peak position is an indication for the different back bonding structures of the Si–H bonds. The narrowing Si–H peak and the converging peak position to  $\sim 2180\text{ cm}^{-1}$  suggest that Si–H bonds with one Si and two N back bonding atoms are thermally most stable. However, more work should be done to clarify this topic.

## 5. Conclusion

A thermal annealing experiment has been conducted on a series of a-SiN<sub>x</sub>:H samples with different N/Si atom ratios deposited by HWCVD. Three different types of evolution behaviors were observed for the a-SiN<sub>x</sub>:H samples, depending on their N/Si atom ratios. Bonded H atoms in more N-rich samples are usually more stable upon thermal annealing.

## Acknowledgment

The research described in this paper was financially supported by the Netherlands Agency for Energy and the Environment (SenterNovem).

## References

[1] A.G. Aberle, Sol. Energy Mater Sol. Cells 65 (2001) 239.

- [2] W. Soppe, H. Rieffe, A.W. Weeber, Prog. Photovolt.: Res. Appl. 13 (2005) 551.
- [3] I.G. Romijn, W.J. Soppe, H.C. Rieffe, A.R. Burgers, A.W. Weeber, in: Proceedings of the 20th European Photovoltaic Solar Energy Conference and Exhibition, Barcelona, Spain, 6–10 June, 2005, p. 1352.
- [4] H.F.W. Dekkers, L. Carnel, G. Beaucarne, Appl. Phys. Lett. 89 (2006) 013508.
- [5] H. Mäckel, R. Lüdemann, J. Appl. Phys. 92 (2002) 2602.
- [6] J. Hong, W.M.M. Kessels, W. Soppe, A. Weeber, W.M. Arnoldbik, M.C.M. van der Sanden, J. Vac. Sci. Technol. B 21 (2003) 2123.
- [7] V. Verlaan, C.H.M. van der Werf, Z.S. Houweling, I.G. Romijn, A.W. Weeber, H.F.W. Dekkers, H.D. Goldbach, R.E.I. Schropp, Prog. Photovolt.: Res. Appl. 15 (2007) 563.
- [8] Z. Lu, P. Santos-Filho, G. Stevens, M.J. Williams, G. Lucovsky, J. Vac. Sci. Technol. A 13 (1995) 607.
- [9] C. Savall, J.C. Bruyere, J.P. Stoquert, Thin Solid Films 260 (1995) 174.
- [10] F.L. Martinez, I. Martil, G. Gonzalez-Diaz, B. Selle, I. Sieber, J. Non-Cryst. Solids 227–230 (1998) 523.
- [11] R.E.I. Schropp, K.F. Feenstra, E.C. Molenbroek, H. Meiling, J.K. Rath, Philos. Mag. B 76 (1997) 309.
- [12] W.M. Arnold Bik, F.H.P.M. Habraken, Rep. Prog. Phys. 56 (1993) 859.
- [13] L.C. Feldman, J.W. Mayer, in: Fundamentals of Surface and Thin film analysis, PTR Pentice-Hall Inc., Upper Saddle River, NJ, USA, 1986.
- [14] M.H. Brodsky, M. Cardona, J.J. Cuomo, Phys. Rev. B 16 (1977) 3556.
- [15] N. Maley, Phys. Rev. B 46 (1992) 2078.
- [16] V. Verlaan, Z.S. Houweling, C.H.M. van der Werf, H.D. Goldbach, R.E.I. Schropp, Jpn. J. Appl. Phys. 46 (2007) 1290.
- [17] Z. Yin, F.W. Smith, Phys. Rev. B 43 (1991) 4507.
- [18] V. Verlaan, C.H.M. van der Werf, W.M. Arnoldbik, H.D. Goldbach, R.E.I. Schropp, Phys. Rev. B 73 (2006) 195333.
- [19] E. Bustarret, M. Bensouda, M.C. Habrard, J.C. Bruyere, S. Poulin, S.C. Gujrathi, Phys. Rev. B 38 (1988) 8171.